

Hydration Effects Accompanying the Substitution of Counterions in the Ionic Atmosphere of Poly(rA)•Poly(rU) and Poly(rA)•2Poly(rU) Helices

Vitaly Buckin, Huy Tran, Victor Morozov, and Luis A. Marky*

Contribution from the Department of Chemistry, New York University,
New York, New York 10003

Received January 24, 1996[⊗]

Abstract: The physical properties of nucleic acid helices strongly depend on their interaction with counterions and water. Of special interest is the structure of their ionic atmosphere which is closely related to its overall hydration because the distances between counterions and the atomic groups of a helix are comparable to the size of a water molecule. In an effort to answer whether the putative higher linear charge density of triple helices, relative to duplexes, exerts special effects on the structural and hydration parameters of their ionic atmosphere, we used a combination of high-precision ultrasonic velocity and density techniques to follow the hydration effects upon substituting Na⁺ for Cs⁺ or Mg²⁺ ions in the ionic atmosphere of poly(rA)•2poly(rU) and poly(rA)•poly(rU). The titration of the Na⁺ salt of each helix with Cs⁺ results in marginal hydration effects. This indicates that both Na⁺ and Cs⁺ form outer-sphere counterion–RNA complexes, where the counterion keeps its coordinated water molecules. The substitution of Na⁺ for Mg²⁺ results in positive compressibility values (3×10^{-4} cm³/bar per mol of nucleotide) and volume effects (2 cm³ per mol of nucleotide), and reflects a small dehydration of the whole Mg²⁺–RNA complexes. The overall dehydration level corresponds to the formation of outer-sphere complexes, indicating that Mg²⁺ keeps most of its coordinated water in the ionic atmosphere of each helical structure. The resulting small effects in the hydration parameters of the triplex ionic atmosphere suggest that the structure of the counterion–triplex complex may be determined by short-range interactions, including the immobilization of water molecules, while the long-range electrostatic interactions that determine the condensation of counterions do not show a significant influence on the local structure of the ionic atmosphere of these helices.

Introduction

The physicochemical properties of nucleic acids depend on their polyelectrolyte behavior, which is determined by the interaction of counterions with the regular lattice of negatively charged phosphate groups of the sugar–phosphate backbone.^{1–3} Therefore, in order to understand how nucleic acids carry out their biological functions, it is necessary to have a complete physical description of these interactions. The simple electrostatic association of monovalent counterions with the ionic atmosphere of DNA duplexes is delocalized, and the cations keep their hydration shell intact^{1,4,5} while the observed dehydration effects in the association of divalent cations like Mg²⁺ are sequence dependent. This has led us to postulate that Mg²⁺ recognizes the sequence of DNA through its overall hydration state, by forming outer-sphere Mg²⁺–nucleotide complexes with dA•dT base pairs and inner-sphere complexes with dG•dC base pairs.⁶

There is renewed interest in investigating triple helices because these novel structures have been implicated as a possible means of controlling cellular processes by endogenous or exogenous mechanisms,^{7–10} but relatively little is known about their polyelectrolyte behavior. The formation of a triple helix,

relative to a duplex, takes place at higher salt concentration. This is due to its higher linear charge density;¹ the repulsions between the negative phosphate charges are stronger so additional Coulombic screening is required by the surrounding atmosphere of counterions. Also, the stronger electric field around a triple helix relative to a double helix leads to a stronger attraction between the triplex and surrounding counterions. Does this result in fundamental differences in the structure of the ionic atmosphere of a triplex relative to a duplex? Are monovalent counterions site bound; and will they lose their hydration shell on contact to the surface of a triplex? Answers to these questions provide our motivation for determining the differences in the binding behavior of counterions to a triplex structure relative to its counterpart duplex.

Furthermore, the distances between the nucleic acid surface and its counterions are comparable to the size of a water molecule.¹ Therefore, the problem of nucleic acid–counterion interactions cannot be analyzed separately from the phenomenon of nucleic acid hydration. However, measurements of hydration effects on counterion binding give information on the structural characteristics of the ionic atmosphere of nucleic acid helices. These hydration changes are determined by the position of the counterion relative to the atomic groups at the nucleic acid surface because of the overlapping of their hydration shells.^{6,11} High-precision ultrasonic velocity measurements are very sensitive for investigations of the hydration properties of a wide range

* To whom correspondence should be addressed.

⊗ Abstract published in *Advance ACS Abstracts*, July 1, 1996.

(1) Manning, G. Q. *Rev. Biophys.* **1978**, *11*, 179.

(2) Record, M. T.; Anderson, C. F.; Lohman, T. M. Q. *Rev. Biophys.* **1978**, *11*, 103.

(3) Pezzano, H.; Podo, F. *Chem. Rev.* **1980**, *80*, 365.

(4) Sisoëff, I.; Grisvard, J.; Guille, E. *Prog. Biophys. Mol. Biol.* **1976**, *31*, 165.

(5) Braulin, W. In *Advances in Biophysical Chemistry*; Bush, C. Allen, Ed.; JAI Press: London, 1995; Vol. 5, pp 89–139.

(6) Buckin, V. A.; Kankiya, B. I.; Rentzeperis, D.; Marky, L. A. *J. Am. Chem. Soc.* **1994**, *116*, 9423.

(7) Le Doan, T.; Perrouault, L.; Chassignol, M.; Thoung, N. T.; Hélène, C. *Nucleic Acids Res.* **1987**, *15*, 8643.

(8) Moser, H. E.; Dervan, P. B. *Science* **1987**, *238*, 645.

(9) Roberts R. W.; Crothers, D. M. *Science* **1992**, *258*, 1463.

(10) Radhakrishnan, I.; Patel, D. J. *Biochemistry* **1994**, *33*, 11405.

(11) Buckin, V. A.; Kankiya, B. I.; Sarvazyan, A. P.; Uedaira, H. *Nucleic Acids Res.* **1989**, *17*, 4189.

of solute molecules.^{12,13} The application of these types of acoustical measurements in determining the physical state of water in the hydration shell of nucleic acids¹⁴ and their components^{11,15} as well as the binding of metal ions⁶ and ligands^{16,17} to DNA has been previously demonstrated.

In this work, we have investigated the influence of the linear charge density on the structural and hydration parameters of the ionic atmosphere of double and triple helices. We used a combination of ultrasonic velocity and solution density measurements to follow the hydration effects accompanying the binding of Cs⁺ and Mg²⁺ to poly(rA)·2poly(rU) and poly(rA)·poly(rU). Specifically, we measured the change of the concentration increment of ultrasonic velocity of polynucleotide solutions, containing Na⁺ in their ionic atmosphere, during the course of titration with Cs⁺ or Mg²⁺. Together with density measurements, we obtained the volume and compressibility effects for these counterion substitutions. We used circular dichroism and UV absorption techniques to follow the changes in base-pair (or base triplet) stacking interactions and force field microscopy to obtain direct information on the structure and conformation of these molecules.

Materials and Methods

Materials. The sodium salts of poly(rA)·poly(rU) and poly(rA)·2poly(rU), designated as duplex and triplex, respectively, were purchased from Sigma. The average length of these helices was 1075 base pairs (duplex) and 220 base triplets (triplex). Each sample was dissolved in 2 mM HEPES buffer, 20 mM NaBr, and 10 mM Na₂EDTA at pH 7.6, dialyzed against the same buffer (without Na₂EDTA) for 48 h, and filtered through Spartan 3–5- μ m filters (Schleicher & Schuell). Their concentration was measured optically at 260 (duplex) or 257 nm (triplex) and 20 °C using the following extinction coefficients (in phosphate): 8.98 (duplex) and 5.9 mM⁻¹·cm⁻¹ (triplex). We used UV melting and differential scanning calorimetry techniques to characterize the helix–coil transition of each helical structure. These curves yielded highly cooperative transitions indicating narrow molecular weight distributions. The HEPES free acid, Na-HEPES, and MgCl₂ were purchased from Sigma, CsCl and NaBr (suprapure grade) and CsOH from Aesar, and NaCl (pure grade) from Fisher. All solutions were prepared with deionized distilled water.

Experimental Conditions. All initial solutions, for measurement, were prepared in 2 mM HEPES buffer and 20 mM NaBr at pH 7.6 and 20 °C. The low ionic strength of this buffer minimizes its contribution to the density. NaBr was selected as supporting electrolyte over NaCl because of its smaller contribution to the value of ultrasonic velocity. At 20 °C, both polynucleotide samples are completely in their helical states, for instance, the thermal denaturation curve of the less stable triplex shows a transition temperature of 31 °C. These experimental conditions optimize the overall precision of the acoustical and density measurements.

Density Measurements. The density of all solutions was measured with an Anton Paar (Graz, Austria) DMA densitometer in the differential mode using two 602-M micro cells (the volume of each cell is 150 μ L). The reference cell was filled with water while the measuring cell was filled with solution or buffer. The temperature was set at 20 °C (± 0.01) and yielded a temperature difference between the

cells of better than a millidegree. The precision of the density measurement, including the reproducibility of refilling the cell, is ± 2 μ g/cm³.

The density, ρ , was calculated from the oscillation period T of the cell by using the following relation: $\rho = AT^2 + B$, where A and B are constants determined from the calibrating densities (and periods) of water and air. The apparent molar volumes of each sample were calculated from the equation¹⁸ $\Phi_v = M/\rho_0 - (\rho_0 - \rho)/\rho_0 c$, where M is the molecular mass of a nucleotide and ρ_0 and ρ are the densities of the solvent and solution, respectively. The volume increment for a two-component mixture (1 and 2) expressed as $\Delta V (=V_{12} - V_1 - V_2)$ per mole of component 1 was calculated from the relation:

$$\Delta V = (c_1 \rho_{12})^{-1} \{ [\rho_1 - \rho_{12}] + [\rho_2 - \rho_{12}] (m_2/m_1) (\rho_1/\rho_2) \} \quad (1)$$

where ρ_{12} , ρ_1 , and ρ_2 are the densities of the mixture and solutions of component 1 and component 2, respectively; c_1 is the concentration of the solution of component 1, and m_1 and m_2 are the masses (in moles) of components 1 and 2 of the mixture. The precision in these measurements is mainly determined by the relative density differences: $[\rho_1 - \rho_{12}]$ and $[\rho_2 - \rho_{12}]$. To prevent evaporation, the mixing of polynucleotide and counterion solutions was done with gas-tight Hamilton syringes through small holes in the caps of narrow 400- μ L plastic tubes. To obtain the change in apparent molar volume, $\Delta\Phi_v$, the resulting ΔV values were corrected for the volume effects of dilution.

Ultrasonic Velocity Measurements. The ultrasonic velocity measurements were performed using the resonator technique,^{19,20} consisting of two plain parallel resonator quartz cells with a volume of 0.4 mL, each attached to lithium niobate piezo-transducers.²¹ The first piezo-transducer converts the sinusoidal electrical signal into an ultrasonic wave of compressions and decompressions that passes through the liquid and then is detected by the second piezo-transducer. Resonance occurred at frequencies corresponding to integer number of one-half of the ultrasonic wavelength between the cell walls, which are determined by measuring the amplitude and phase shift. The difference between the ultrasonic velocity of the solutions and water (used as reference) was obtained from the resonances frequencies of the sample cell by the relation:

$$(u - u_0)/u_0 = [(f - f_0)/f_0](1 + \gamma) \quad (2)$$

where f and f_0 are the frequencies corresponding to the maxima of the resonance peaks of a selected resonance harmonic of the cells filled with solution and water, respectively; γ is a small constant of $\sim 10^{-2}$ determined by calibration with NaCl. The instrument has been programmed as follows: first one determines the position of the selected resonance peak by performing amplitude decay measurements and then one determines the exact frequency, for which the phase shift between the input and output signals of the cell achieved a set value. This frequency corresponds to the maximum amplitude of the resonance peak and was used as f or f_0 in eq 2. All measurements were performed in the frequency range of 6.5–6.6 MHz. The relative error in the measurement of $(u - u_0)/u_0$ is $\pm (2 \times 10^{-5})\%$, which is mainly determined by the constancy of the solution composition. Another important factor is evaporation, which changes the concentration of buffer and thus the ultrasonic velocity; for instance, the contribution of NaCl to the ultrasonic velocity using a 50 mM NaCl solution is 11 times higher than that of a 2 mM (in nucleotide) polynucleotide solution. To measure the polynucleotide contribution with a precision of 1%, extreme precautions were taken to keep evaporation below 0.1%. Therefore, in the Cs⁺ titrations we used as a titrant a buffer solution of a 1:1 mixture of Cs-HEPES/H-HEPES (0.12 M) and 1.83 M CsCl, at 20 °C; under these conditions the value of the ultrasonic velocity for this solution is similar to that of water. The titration of 400- μ L polynucleotide solutions with Cs⁺ or Mg²⁺ was performed by stepwise additions of 4- μ L aliquots of titrant solution using calibrated Hamilton syringes. Complete mixing was effected with a stainless steel vibrating stirrer.

(18) Millero, F. J. In *Water & Aqueous Solutions*, Horne, R. A., Ed., Wiley-Interscience, New York, 1972; pp 519–595.

(19) Eggers, F.; Funck, Th. *Rev. Sci. Instrum.* **1993**, *44*, 969.

(20) Sarvazyan, A. P. *Ultrasonics* **1982**, *20*, 151.

(21) Buckin, V. A.; De Maeyer, L.; Funck Th., PCT application, WO 94/24526, October 27, 1994.

(12) Conway, B. E. In *Ionic Hydration in Chemistry and Biophysics*; Elsevier: New York, 1981.

(13) Hoiland, H. In *Thermodynamic Data for Biochemistry and Biotechnology*; Springer-Verlag: Berlin-Heidelberg, 1986; pp 129–147.

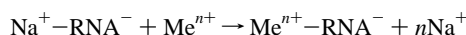
(14) Buckin, V. A.; Kankiya, B. I.; Bulichov, A. V.; Lebedev, A.; V.; Gukovsky, I. Ya.; Chuprina, V. P.; Sarvazyan, A. P.; Williams, A. R. *Nature* **1989**, *30*, 321.

(15) Buckin V. A. *Biophys. Chem.*, **1988**, *29*, 283.

(16) Buckin, V. A.; De Maeyer, L.; Funck Th.; Kudrjashov, E.; Braginskaya, F.; Kankiya, B. I.; Marky, L. A. *J. Biomol. Struct. Dynam.* **1993**, *10*, a21.

(17) Chalikian T. A.; Plum, G. E.; Sarvazyan, A. P.; Breslauer, K. J. *Biochemistry* **1994**, *33*, 8629.

Background of Ultrasonic Measurements. The apparent molar volume, Φ_v , is defined as the change in volume upon dissolution of n_2 moles of a solute in an initial volume V_0 of buffer ($\Phi_v = (V - V_0)/n_2$); a similar definition is used for the apparent molar adiabatic compressibility, Φ_{ks} ($\Phi_{ks} = (K - K_0)/n_2$), where $K (= -(\partial V/\partial P)_S)$ and $K_0 (= -(\partial V_0/\partial P)_S)$ are the adiabatic compressibilities of the solution and buffer, respectively (P is the pressure and S is the entropy). Since volume is an additive property of a system, Φ_v for dilute solutions can be expressed by $\Phi_v = V_m + \Delta V_h$, where V_m is the intrinsic volume of the solute molecule that is inaccessible to the surrounding solvent (water) molecules and ΔV_h is a hydration term that corresponds to the difference in the volume of the solute hydration shell and that of the same quantity of pure water. Thus, ΔV_h is determined by the change in the volume of water of the hydration shell plus the void volume between the solute molecule and surrounding solvent. In a similar way, Φ_{ks} is given by¹⁵ $\Phi_{ks} = K_m + \Delta K_h + K_r$, where K_m is the intrinsic compressibility (corresponding to V_m), ΔK_h represents the difference in the compressibility of the hydration shell and that of an equivalent mass of pure water, and K_r is the relaxation compressibility, resulting from temperature and pressure perturbations of the ultrasonic wave. For nucleic acid helices, the magnitude of K_m remains small and nearly constant while K_r can be neglected because it is relatively much smaller than ΔK_h .¹¹ Therefore, $\Delta\Phi_v$ and $\Delta\Phi_{ks}$ for the reaction:



are determined mainly by their hydration contributions:

$$\Delta\Phi_v = \Delta(\Delta V_h) \quad (3)$$

$$\Delta\Phi_{ks} = \Delta(\Delta K_h) \quad (4)$$

In this work, we use density measurements to obtain the $\Delta\Phi_v$ values for the substitution of Na^+ for Cs^+ or Mg^{2+} in the ionic atmosphere of poly(rA)·poly(rU) and poly(rA)·2poly(rU) directly. The $\Delta\Phi_{ks}$ values can be obtained from the volume and ultrasonic velocity measurements using the equation:

$$\Phi_{ks} = 2\beta_0(\Phi_v - A - M/2\rho_0) \quad (5)$$

where β_0 and ρ_0 are the compressibility and the density of the solvent, respectively, A is the concentration increment of ultrasonic velocity and is determined by $A = (u - u_0)/(u_0\rho_0m)$, u and u_0 are the ultrasonic velocities of the solution and solvent, respectively, and m is the molar concentration. In dilute solutions, if the density of the solution is similar to that of the solvent then A reduces to $A = (u - u_0)u_0c$, where c is the molarity of the solute. In experiments where the solvent parameters (β_0 and ρ_0) are nearly constant, i.e., the $\text{Na}^+ - \text{Mg}^{2+}$ substitution experiments, the changes in A at saturation result from the changes in Φ_v and Φ_{ks} :

$$\Delta A = \Delta\Phi_v - \Delta\Phi_{ks}/2\beta_0 \quad (6)$$

In the titrations with Cs^+ that resulted in concentrated solutions of salt, the changes in the density and compressibility of the solvent contribute significantly to ΔA . To exclude this contribution, the measured change in the concentration increment of ultrasonic velocity, δA , was corrected for the changes in the solution density and compressibility. The δA_{corr} as a function of salt concentration is given by the relation: $\delta A_{\text{corr}} = \Phi_{ks}/(2\beta_0[\text{salt}]_{\text{init}}) + M/(2\rho_0[\text{salt}]_{\text{init}}) - \Phi_{ks}/(2\beta_0[\text{salt}]) - M/(2\rho_0[\text{salt}])$, where the terms $\beta_0[\text{salt}]_{\text{init}}$ and $\rho_0[\text{salt}]_{\text{init}}$ are the initial coefficient values of adiabatic compressibility and density for the buffer while the $\beta_0[\text{salt}]$ and $\rho_0[\text{salt}]$ terms refer to finite salt concentrations. Therefore, the corrected value of ultrasonic velocity increment $\delta A'$ ($=\delta A_{\text{exp}} - \delta A_{\text{corr}}$) will reflect just the change of apparent molar volume and apparent molar adiabatic compressibility for the overall association of counterions to a nucleic acid helix.

UV Absorption Spectroscopy. The spectrum of each counterion-helical complex at different $[\text{Me}^{n+}]/[\text{P}]$ molar ratios was obtained on a Perkin-Elmer 552 spectrophotometer equipped with a thermoelectrically controlled cell holder and interfaced to a PC computer for acquisition and analysis of experimental data. These spectra allowed definition of the global conformational state of each helical sample and verification of the formation of equilibrium states in low and high concentration of counterions by the presence of isosbestic points at different

[counterion]/[helix] molar ratios. Spectroscopic titrations of each helix were performed at 260 and 280 nm by stepwise addition of 1–30- μL aliquots (depending on the cell volume) of a concentrated counterion solution, using a Hamilton syringe, directly to a quartz cell containing the polynucleotide, and the cell content was mixed by manual shaking. After each addition, the absorbance was followed as a function of time until an equilibrium value is reached—up to 2 h for low salt solutions and a few minutes for high salt solutions. Some curves yielded a short relaxation process in the initial 5-min period followed by a longer relaxation that lasted up to 150 min. For the analysis of these kinetic curves, the experimental data of the second relaxation were fitted with simple exponential functions to determine their amplitudes and characteristic half-times.

Circular Dichroism (CD) Spectroscopy. All CD spectra were obtained on an AVIV-60DS spectrometer equipped with a Hewlett-Packard thermoelectrically controlled cell holder. Each spectrum corresponds to an average of three scans between 330 and 200 nm using 1 nm steps.

Scanning Force Microscopy. Polynucleotide samples with or without Mg^{2+} were prepared using nickel-treated mica as described previously.²² Freshly cleaved mica surface was treated for a few seconds with a 1–3 mM NiCl_2 solution, thoroughly rinsed with double distilled water, and blow dried with compressed nitrogen. Immediately before each deposition, a 0.4 mM polynucleotide solution (in phosphate) was diluted ~200-fold with buffer and 2–3 μL of solution were applied onto the surface for 5–20 s, rinsed with water, and blow dried with nitrogen. The images on this surface were obtained using a Digital Instruments Nanoscope II equipped with a 10- μm nanoprobe head. Scanning was performed in a closed chamber filled with dry air or nitrogen, using commercial nanotips with a spring constant of 0.03 N/m from Digital Instruments Inc. (Santa Barbara, CA). Both types of “force” and “high” scanning modes were used. The scanning rate varied from 7 to 18 Hz and the tip force was minimized by adjusting the setpoint of the optical readout signal to a minimum value; this corresponded to a cantilever bending force of about 1 nN.²³

Results

UV Titrations of Poly(rA)·Poly(rU) with Cs^+ and Mg^{2+} .

The titration curve of this duplex with Cs^+ by monitoring the absorbance at 260 and 280 nm (Figure 1a) shows a decrease in the absorbance upon increasing the salt concentration. In the range of 0–200 of $[\text{Cs}^+]/[\text{P}]$, the absorbance drops 4% at 260 nm and remains nearly constant at 280 nm, while in the range of 200–500 $[\text{Cs}^+]/[\text{P}]$ the absorbance at 260 nm decreases an additional 1% and drops 3% at 280 nm. It has been shown that the 260-nm optical window monitors the formation of duplex from the mixing of two complementary strands while the one at 280 nm follows the formation of triplex through a disproportionation reaction of two duplexes.²⁴ Consistent with these observations, our results show that additional formation of base-pair stacks takes place in the first region while some triplex forms in the latter one. This conclusion is in agreement with the reported phase diagrams of poly(rA) and poly(rU) mixtures in NaCl and KCl.^{24,25}

Similar absorbance changes are detected upon binding of Mg^{2+} to the same duplex (Figure 1b). However, at both wavelengths a similar decrease of the absorbance takes place in the $[\text{Mg}^{2+}]/[\text{P}]$ molar ratio of 0–0.5 with a plateau between 0.3 and 0.7 $[\text{Mg}^{2+}]/[\text{P}]$ ratios. Above the $[\text{Mg}^{2+}]/[\text{P}]$ ratio of 0.7, the decrease in the absorbance is 2% at 260 nm and 4% at 280 nm. This indicates that Mg^{2+} binding is more effective on inducing conformational perturbations.

UV Titrations of Poly(rA)·2poly(rU) with Cs^+ and Mg^{2+} .

The spectra of the triplex in the presence of several Cs^+ (or

(22) Bezanilla, M.; Drake, B.; Nudler, E.; Kashlev, M.; Hansma, P. K.; Hansma, H. G. *Biophys. J.* **1994**, *67*, 2454.

(23) Shaper, A.; Starink, J. P.; Jovin, T. *FEBS Lett.* **1994**, *335*, 91.

(24) Stevens, C. L.; Felsenfeld, G. *Biopolymers* **1964**, *2*, 293.

(25) Krakauer, H.; Sturtevant, J. M. *Biopolymers* **1968**, *6*, 491.

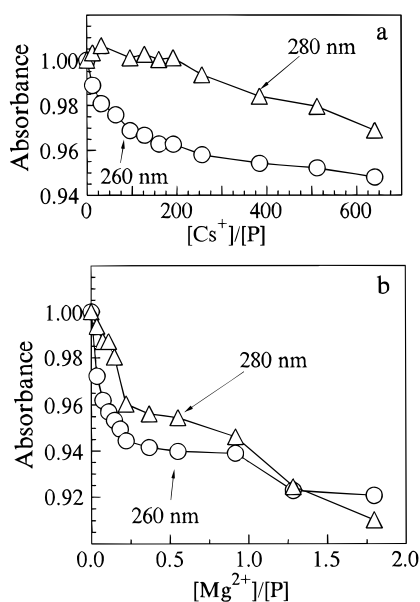


Figure 1. UV titrations of poly(rA)·poly(rU) with CsBr (a) and $MgBr_2$ (b) at 260 (circles) and 280 nm (triangles) in 2 mM Na-HEPES and 20 mM NaBr at pH 7.6 and 20 °C. The absorbance values have been corrected for dilution and normalized by the initial absorbance. The concentration of polynucleotide is 1 mM (in phosphate).

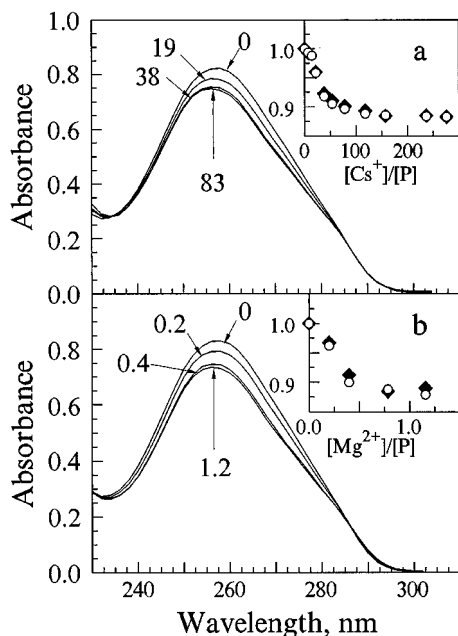


Figure 2. Typical UV spectra of poly(rA)·2poly(rU) in 2 mM Na-HEPES and 20 mM NaBr at pH 7.6 and 20 °C, and at the indicated molar ratio of counterion to polynucleotide: CsBr (a) and $MgBr_2$ (b). The concentration of polynucleotide is 1 mM (in phosphate). Insets: Resulting optical titrations at 257 (circles) and 280 nm (squares).

Mg^{2+}) concentrations are shown in Figure 2a,b, and the resulting optical titration curves at 257 and 280 nm, respectively, are shown in the insets. The overlay of the spectra for each counterion shows the presence of a clear isobestic point at 286 nm that indicates the presence of an equilibrium between two conformational states. The CD spectra of these two states at different Cs^+ concentrations (data not shown) correspond to a triplex in the characteristic A-conformation. However, the spectra at high Cs^+ concentration is shifted to shorter wavelengths; the wavelength of maximum ellipticity at 257 nm has been shifted ~ 10 nm. The optical titration curves also show that counterion binding lowers the absorbance but, contrary to

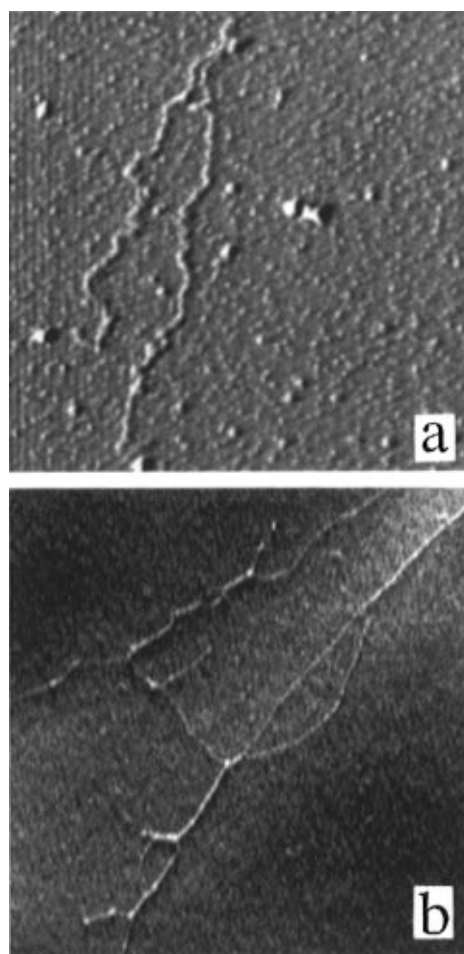


Figure 3. Typical scanning force microscope images of polynucleotides in 2 mM Na-HEPES and 20 mM NaBr at pH 7.6. These images were obtained in dry air after deposition on mica surface: (a) poly(rA)·poly(rU) with an image size of 650 × 650 nm. (b) poly(rA)·2poly(rU) with an image size of 4500 × 4500 nm.

the titrations of the duplex, the curves at both wavelengths (257 and 280 nm) are similar for each counterion. For Cs^+ , the 12% drop in absorbance takes place in the $[Cs^+]/[P]$ range of 0–200 and remains nearly constant to a $[Cs^+]/[P]$ value of 600. For Mg^{2+} , similar changes in hypochromicity take place, but the curves are shifted to much lower $[Mg^{2+}]/[P]$ ratios.

An additional observation is that the observed spectral changes for the triplex are slow, with half-times of 10 to 60 min depending on the concentration of salt. To assure that the starting sample solutions were similar, i.e., at equilibrium, sample solutions were dissolved in low and high salt buffer and dialyzed against the low salt buffer. Then each sample was used in the titration experiments with salt. These samples yielded similar titration curves.

The overall optical results indicate that binding of each counterion is favoring the formation of more base-triplet stacks *via* monomolecular or multimolecular processes. To distinguish between these two possibilities, kinetic experiments were carried out over a 10-fold triplex concentration (data not shown). These experiments show that the overall hypochromicities and half-lives depended on the concentration of triplex and indicate that the local and additional formation of base-triplet stacks most likely takes place in bimolecular processes.

Scanning Force Microscopy. Figure 3a shows a typical image for the duplex in the presence of Mg^{2+} ; similar images were obtained for each of the two component single strands

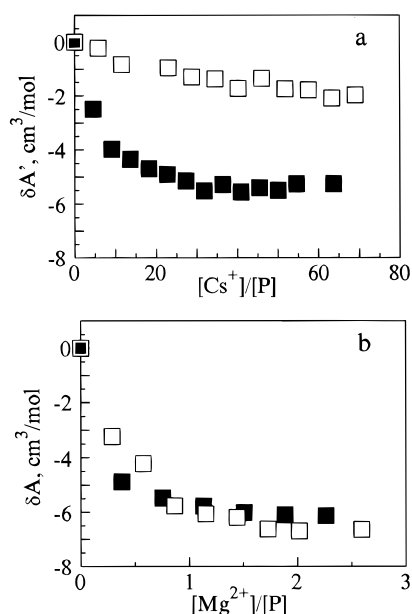


Figure 4. Acoustical titrations of poly(rA)·poly(rU) (open squares) and poly(rA)·2poly(rU) (closed squares) in 2 mM Na-HEPES and 20 mM NaBr at pH 7.6 at 20°C, with Cs⁺ (a) and Mg²⁺ (b). The $\delta A'$ values of the Cs⁺ titrations have been corrected for the high salt concentration used (see text). The concentration of polynucleotide was 3–5 mM (in phosphate).

and for the triplex. The main difference among the images of these four molecules are their heights: 0.4 (poly(rA) or poly(rU)), 0.6 (duplex), and 0.9 nm (triplex). This is in good agreement with previous images of double- and single-stranded DNA molecules.^{26–28} In the images of the triplex, sections can be seen in which different triple helices were connected to each other (Figure 3b), while in the absence of Mg²⁺ this connectivity is enhanced. In the duplex image, the number of associated duplexes is much lower.

Ultrasonic Titration Curves. Due to the high CsCl concentrations used in the ultrasonic titrations, the δA_{exp} values have been corrected for the changes in solution density (and compressibility) with salt concentration. The $\rho_o[CsCl]$ values were obtained from the literature¹⁸ while the values of $\beta_o[CsCl]$ were calculated from our ultrasonic velocity data using the well known relation for the coefficient of adiabatic compressibility, β : $\beta = 1/(u^2\rho)$. In the acoustical titrations with Mg²⁺, no corrections were necessary because of the much lower concentrations of MgBr₂ used. Figure 4a shows the resulting ultrasonic titration ($\delta A'$ as a function of the molar ratio $[Me^{n+}]/[P]$) for each helix with Cs⁺ and Figure 4b the corresponding titrations with Mg²⁺. All four curves show similar shapes; increasing the counterion concentration results in a decrease of $\delta A'$ that levels off at $[Me^{n+}]/[P]$ ratios of 50 for Cs⁺ and 2 for Mg²⁺. At these saturating ratios, the resulting $\delta A'$ values correspond to the overall hydration changes that take place upon substituting Na⁺ for Cs⁺ (or Mg²⁺) in the ionic atmosphere of each helix. The saturating $\delta A'$ values varied with both the nature of counterion and helix used; see Table 1.

The Volume and Compressibility Effects of Counterion Binding. The volume effects ($\Delta\Phi_v$) of Mg²⁺ binding to each helix are given in Table 1, and these values correspond to the plateaus of the ultrasonic titration curves. These values

together with the ΔA values allow us to calculate, using eq 5, the change in apparent molar adiabatic compressibility ($\Delta\Phi_{ks}$) for the same interactions. Both the volume and compressibility effects of Mg²⁺ binding to each helical structure are positive and indicate a decrease in the overall hydration level of the entire system composed of counterion and polynucleotide. This is because the molar volume and compressibility of the water surrounding nucleic acids is lower than bulk water.^{11,14} In general, the binding of counterions to a nucleic acid results in two hydration contributions to the volume and compressibility effects, which are due to conformational perturbations of the polynucleotide and to the coordination of counterion with atomic groups at the surface of the nucleic acid. A detailed analysis of these contributions will be discussed in a later section, but it is important to emphasize that the resulting absolute values of the volume and compressibility effects for the interaction of each counterion to the duplex and triplex are small and show no fundamental differences in the structure of the complexes of counterion with each helix.

Discussion

For a direct comparison of the observed optical and acoustical changes that take place in the binding of counterions to each helical structure, the two types of observables have been superimposed by adjusting their scales. An adjusting coefficient of 50 cm³/mol per absorbance unit was applied to the Cs⁺ and Mg²⁺ acoustical titrations. The resulting curves are shown in Figures 5a–c; the Cs⁺ curves superimposed as a function of the total concentration of Cs⁺ while the Mg²⁺ curves are superimposable as a function of the $[Mg^{2+}]/[P]$ ratio. Mg²⁺ binds stronger to each helix; therefore, much lower Mg²⁺ concentrations are needed to induce the observed changes. The main observation is that the relative changes in these two observables are similar and indicate that the nature of both ultrasonic and UV changes results from similar molecular processes, i.e., counterion binding induces conformational changes resulting in hypochromicity and dehydration effects. One exception is the Mg²⁺–duplex curves that deviate at $[Mg^{2+}]/[P] > 0.5$, which is due to the disproportionation reaction of two duplexes to form a triplex and a single strand; as such, the acoustical contribution of each participating specie has to be taken into account.

Conformational Rearrangements in the Interaction of Cs⁺ with Poly(rA)·2Poly(rU) and Poly(rA)·Poly(rU). The observed changes in the UV and CD spectral characteristics indicate conformational rearrangements for each helical structure with the increase in the concentration of CsCl. For the understanding of the type of conformational changes that are taking place and for the nature of these changes, the following experimental facts shall be considered: (i) the resulting hypochromicities for each helix in their titration with salt indicate an increase of base-pair stacking interactions; (ii) the changes in the CD spectra with the increase in the ionic strength are consistent with the additional formation of base-pair stacks, as observed earlier;²⁹ (iii) the presence of isosbestic points in the UV spectra of the triplex suggests an equilibrium of two conformers; and (iv) the acoustical and optical titrations are superimposable for each helix. From the resulting changes in absorbance of 4% (duplex) and 11% (triplex) of these experiments and the total hyperchromicity of 35% (duplex) and 40% (triplex) obtained in UV melting curves for these helices, we estimate that 8% (duplex) and 20% (triplex) of open base pairs are being closed upon increasing the Cs⁺ (or Na⁺, data not shown) concentration to 0.2 M. In the duplex, the presence of

(26) Bustamante, C.; Keller, D.; Yang, G. *Curr. Opin. Struct. Biol.* **1993**, *3*, 363.

(27) Thundat, T.; Allison, D. P.; Warmack, R. J.; Doktycz, M. J.; Jacobson, K. B.; Brown, G. M. *J. Vac. Sci. Technol.* **1993**, *11*, 824.

(28) Lyubchenko, Y. L.; Shlakhtenko, L.; Harrington, R.; Oden, P.; Lindsay, S. *Proc. Natl. Acad. Sci. U.S.A.* **1993**, *90*, 2137.

(29) Brams, J. *J. Mol. Biol.* **1965**, *11*, 785.

Table 1. Volume, Compressibility, and UV Changes on the Binding of Cs⁺ and Mg²⁺ to RNA Polynucleotides^a

polymer	[Mn ⁿ⁺]/[P]	$\Delta\Phi_v$, cm ³ /mol	$10^4\Delta\Phi_{ks}$, cm ³ /(mol·bar)	ΔA , cm ³ /mol	Δ absorbance, ^b %
Magnesium					
poly(rA)·poly(rU)	2.0	1.6	7.6	-6.7	-8
poly(rA)·poly(rU)	0.5		4.7 ^c	-3.5	-6
poly(rA)·2poly(rU)	2.0	2.2	7.5	-6.0	-13
Cesium					
poly(rA)·poly(rU)	~50			-1.9	-4
poly(rA)·2poly(rU)	~50			-5.6	-11

^a Values taken in 2 mM HEPES buffer, 20 mM NaBr at pH 7.6 and 20 °C, and given per mole of phosphate. The concentrations of polynucleotide (in phosphate), indicating experimental uncertainties, were as follows: 6–8 mM and ± 0.6 cm³/mol for $\Delta\Phi_v$ measurements; 3–5 mM and ± 0.3 cm³/mol for the ΔA measurements; 1–1.5 mM and $\pm 0.5\%$ for the UV absorption measurements; and $\pm 0.8 \times 10^{-4}$ cm³/(mol·bar) for the $\Delta\Phi_{ks}$ values. All experimental uncertainties were estimated by error propagation and/or reproducibility of the initial measurements. ^b This is a normalized absorbance at 260 nm, calculated from the titration curves as the ratio of absorbance at saturation to the initial absorbance. ^c This $\Delta\Phi_{ks}$ value was estimated using the $\Delta\Phi_v$ value at $[Mg^{2+}]/[P] = 2$; the volume effect of duplex formation is small. The $\Delta\Phi_v$ values for the binding of Cs⁺ were not measured because of the large contribution of salt to the solution density.

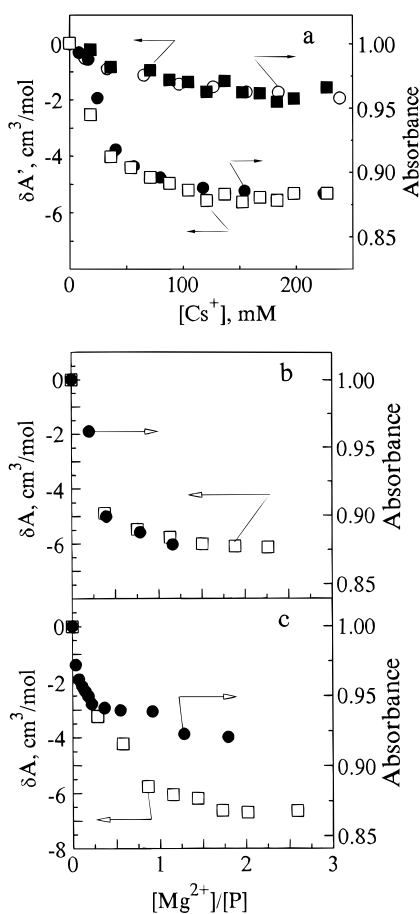


Figure 5. Direct comparison of the acoustical (squares) and optical (circles, at 260 nm) titrations, all four acoustical titrations were superimposed to the optical curves by normalizing their scales with a coefficient of 50 cm³/mol per absorbance unit: (a) Cs⁺–duplex (upper curves) and Cs⁺–triplex (lower curves); (b) Mg²⁺–triplex; (c) Mg²⁺–duplex. All experimental conditions as in Figures 1, 2, and 4.

open base-pairs may be due to the heterogeneity of the single strand lengths resulting in the formation of imperfect helices containing gaps, loops and branches. Increasing the ionic strength favors the formation of base pairs in these open nucleotide segments, through screening effects, yielding a more flexible double helix with a decrease in its effective diameter and excluded volume, which normally takes place at ~ 0.1 M salt. In the triplex, the additional third strand increases both the probability of loop and branch formation with longer lifetimes and the formation of intermolecular complexes as seen in the force scanning microscopy images. The fast kinetic data observed in the titrations of the duplex can be explained in a

similar way: increasing the ionic strength stabilizes the double helical structure by closing base pairs in the loops and branches; however, the slow kinetics observed with the triplex is due to the participation of three strands in the formation of additional base-triplets that need topological rearrangements, including a redistribution of strands.

Another interesting observation is that Cs⁺ is more effective than Na⁺ in closing base-triplets; lower concentrations of Cs⁺ are needed to reach the saturating values and the overall kinetic effects are faster. Since there is no indication that Cs⁺ should interact differently with the triplex, then the most probable explanation for this effect is the differential binding of Cs⁺ and Na⁺ to transient open bases and/or single-stranded segments of these chains.

Hydration Effects in the Substitution of Na⁺ for Cs⁺ in the Triplex Ionic Atmosphere. The observed hydration effects measured in the ultrasonic titrations with Cs⁺ may be the result of two coupled contributions: conformational rearrangements and the actual coordination of Cs⁺ counterions. It is well known that monovalent counterions in the ionic atmosphere of duplexes keep their entire hydration or coordination shell.^{1,5,11} Since the acoustical and optical titration are superimposable, the observed hydration changes are due mainly to conformational rearrangements. In the case of the triplex the two observables also superimpose within the experimental uncertainty of ~ 1 cm³/mol; therefore, the specific substitution of Na⁺ for Cs⁺ in the ionic atmosphere of the triplex does not contribute to the observed hydration changes, and the monovalent counterions like Na⁺ and Cs⁺ are bound to the triplex in the same way as to the duplex, that is the counterion keeps its hydration shell.

The same conclusion can be reached from the analysis of our experimental data, as follows: the measured ΔA values in KCl for the formation of duplex and triplex from the mixing of their component single strands are -15.6 and -15.3 cm³/mol, respectively.³⁰ Therefore, the 8% (duplex) and 20% (triplex) of closed base-pairs will correspond to -1.3 and -3.1 cm³/mol, respectively. The ΔA values for the substitution of Na⁺ for Cs⁺ reported here are -1.9 (duplex) and -5.3 cm³/mol (triplex). Considering the different experimental conditions, these values are in good agreement. In the event that the differences are real and resulting from the specific coordination of counterions, we estimate an average ΔA value of ≤ 2 cm³/mol for the hydration effect of substituting Na⁺ for Cs⁺ in the ionic atmosphere of these helices. This value is relatively small and is consistent with the notion that the binding of monovalent counterions to double helices is delocalized,¹ i.e., the counterions are not site bound, and negligible hydration changes are expected upon their substitution.

Mg²⁺ Is More Effective in Producing the Overall Changes. The overall optical, ultrasonic, and kinetic effects of Mg²⁺ binding to each helix are similar to those of Cs⁺ binding. This indicates that similar effects take place; one difference is that Mg²⁺ is more effective in the Coulombic screening of the negatively charged phosphate groups. As a result much lower concentrations of Mg²⁺ are needed to reach the saturation values in both optical and ultrasonic titration curves, [Mg²⁺]/[P] < 1 for Mg²⁺ (<4 mM in our experiments), while for Cs⁺ and Na⁺ the concentrations needed are in the physiological range of 0.1–0.2 M. The Mg²⁺ acoustical titrations of the triplex and duplex (up to a [Mg²⁺]/[P] ratio of 1), in spite of using similar Mg²⁺ and polynucleotide (in phosphate) concentrations, are also superimposable with the optical curves and suggest that the source of the changes is similar. The Cs⁺ results suggest that the conformational perturbations and accompanied dehydration events resulting from increasing the ionic strength are due entirely to electrostatic effects, which for Mg²⁺ correspond to both the overall electrostatic effect and the coordination of counterions. The latter will be discussed in the next section.

The Hydration Effect of Mg²⁺ Binding to Each Helix Corresponds to the Formation of Outer-Sphere Complexes.

The volume and compressibility effects of Mg²⁺ binding to each helical structure, as well as ΔA , also result from the sum of two contributions: the sole hydration effect of the coordination of Mg²⁺ plus the coupled conformational changes. The latter contribution to the volume effect can be estimated from literature data. The volume effects for the formation of each helix are small and in the range of -1.5 to 3.6 cm³/mol for the duplex and from -0.2 to -2.5 cm³/mol for the triplex.^{30–32} Correcting these values for the contribution of closing the opened base-pairs results in a ΔV value of < 0.5 cm³/mol for the volume effect of Mg²⁺ binding to each helix. This value is within the experimental uncertainty and can be neglected. On the other hand, the conformational contribution to ΔA in the Mg²⁺ titration curves can be estimated from the Cs⁺ titration curves by assuming that these ΔA values, -1.9 (duplex) and -5.3 cm³/mol (triplex), are determined entirely by the conformational reorganization. Therefore, for the sole hydration contribution of the coordination of Mg²⁺ to the triplex, we obtain a final ΔA value of -1.4 cm³/mol per mol of bound Mg²⁺; the volume effect is 4.4 cm³/mol per mol of bound Mg²⁺ and a compressibility of 5.2×10^{-4} cm³/(mol·bar) per mol of bound Mg²⁺. The magnitudes of these values are small and indicate that marginal effects are involved in the substitution of Na⁺ for Mg²⁺ in the ionic atmosphere of the triplex. In addition, since there are no indications that Na⁺ is dehydrated in the ionic atmosphere

of a triplex, we can conclude that Mg²⁺ keeps its coordination water in the ionic atmosphere of the triplex and that outer-sphere type complexes predominate.

For the duplex, the value of ΔA in the first part of Mg²⁺ binding before the duplex to triplex transition is about -3.5 cm³/mol (see Figure 5c). Corrected for the conformational contribution of 1.9 cm³/mol, this results in a ΔA value of -1.6 cm³/mol per mol of phosphate or -3.2 cm³/mol per mol of bound Mg²⁺. For the compressibility effect of the hydration contribution of coordinating Mg²⁺, we obtain 5.9×10^{-4} cm³/(mol·bar) per mol of bound Mg²⁺. As in the case of the triplex, both the ΔA and $\Delta\Phi_{ks}$ correspond to the characteristic values for the formation of outer-sphere complexes.⁶

Conclusions

We found essentially no differences in the type of complexes that Mg²⁺ forms with an RNA duplex or triplex. With each helical structure, Mg²⁺ keeps its coordination water in the ionic atmosphere of the polynucleotide forming outer-sphere complexes. Furthermore, in spite of the higher linear charge density of the triplex, Cs⁺ and Na⁺ do not form inner-sphere complexes in their interaction with nucleic acid helices. One possible explanation is that the structure of a counterion–nucleic acid complex is mainly determined by short-range interactions that include the structural reorganization of hydrating water, which is determined by the structure of the surface of a nucleic acid. The long-range interactions that determine the condensation of counterions around nucleic acids do not show significant influence on the local structure of their ionic atmosphere. This conclusion is in good agreement with our previous data on the binding of Mg²⁺ to oligomers and polymers,⁶ in which the counterion condensation phenomenon inherent in double-helical polynucleotides is absent in short oligonucleotides and yet similar Mg²⁺–nucleotide complexes are observed.

In addition, we report that the solution structure of synthetic polymers is far from ideal especially at low ionic strengths. Therefore, in studies of the physicochemical properties of double and triple helices using synthetic polynucleotides, it is important to use several experimental approaches to find out the real solution structure of the polymers and for the evaluation of the actual contributions of structural nonidealities to the measuring parameters.

Acknowledgment. This work was supported by Grant No. GM-42223 from the National Institutes of Health. The editorial assistance of Professor Louise Pape is greatly appreciated.

JA960256Y

(31) Rentzperis, D.; Kupke, D. W.; Marky, L. A. *Biopolymers* **1993**, *33*, 117.

(32) Noguchi, H.; Arya, S. K.; Yang, J. T. *Biopolymers* **1971**, *10*, 2491.